

## **Spatial optimization of watershed best management practices based on slope position units**

C.-Z. Qin, H.-R. Gao, L.-J. Zhu, A.-X. Zhu, J.-Z. Liu, H. Wu

**Cheng-Zhi Qin** is a professor at the State Key Laboratory of Resources and Environmental Information System, the Institute of Geographic Sciences and Natural Resources Research, the Chinese Academy of Sciences; the University of Chinese Academy of Sciences in Beijing, China; and the Jiangsu Center for Collaborative Innovation in Geographical Information Resource Development and Application in Nanjing, China.

**Hui-Ran Gao** is a graduate student at the State Key Laboratory of Resources and Environmental Information System, the Institute of Geographic Sciences and Natural Resources Research, the Chinese Academy of Sciences; and the University of Chinese Academy of Sciences in Beijing, China.

**Liang-Jun Zhu** (corresponding author) is a Ph.D. student at the State Key Laboratory of Resources and Environmental Information System, the Institute of Geographic Sciences and Natural Resources Research, the Chinese Academy of Sciences; and the University of Chinese Academy of Sciences in Beijing, China.

**A-Xing Zhu** is a professor at the State Key Laboratory of Resources and Environmental Information System, the Institute of Geographic Sciences and Natural Resources Research, the Chinese Academy of Sciences, Beijing, China; the Key Laboratory of Virtual Geographic Environment, Ministry of Education, Nanjing Normal University, Nanjing, China; the Jiangsu Center for Collaborative Innovation in Geographical

Information Resource Development and Application in Nanjing, China; and the Department of Geography, University of Wisconsin-Madison.

**Jun-Zhi Liu** is an associate professor at the Key Laboratory of Virtual Geographic Environment, Ministry of Education, Nanjing Normal University, Nanjing, China; and the Jiangsu Center for Collaborative Innovation in Geographical Information Resource Development and Application, Nanjing, China.

**Hui Wu** is a lecturer at the Smart City Research Center, Hangzhou Dianzi University, Hangzhou, China.

# 1 **Spatial optimization of watershed best management practices based on** 2 **slope position units**

3 **Abstract:** Spatial optimization of best management practices (BMPs) is an effective way to select  
4 and allocate BMPs for watershed management such as soil and water conservation, nonpoint  
5 source pollution reduction, etc. The commonly used spatial units for BMP configuration (or BMP  
6 configuration units) include sub-basins, hydrologic response units (HRUs), farms, and fields.  
7 Normally, these spatial units are not homogeneous functional units from the perspective of  
8 physical geography at the hillslope scale (in terms of geomorphic and hydrologic conditions of the  
9 hillslope, for example), and thus cannot effectively represent the spatial relationships between  
10 BMPs and spatial locations with respect to hillslope processes from upstream to downstream. This  
11 makes it difficult to efficiently and rationally construct spatial optimizations for watershed BMPs.  
12 This paper proposes a spatial BMP optimization approach based on slope position units, which are  
13 homogeneous spatial units with physical geographic features. In the proposed approach, slope  
14 position units are used as BMP configuration units by which the relationships between BMPs and  
15 slope positions along a hillslope can be explicitly considered during BMP scenario initialization  
16 and optimization via genetic algorithm (i.e., NSGA-II). A distributed and physically-based  
17 watershed model was used to evaluate the environmental effectiveness (i.e., the reduction rate of  
18 soil erosion), and a simple estimation method was developed to calculate the net cost of BMP  
19 scenarios. A case study was conducted in a small hilly watershed in the typical red-soil region of  
20 the Fujian province in southeastern China, which suffers severely from soil erosion. A simple  
21 system of three types of slope positions (i.e., ridge, backslope, and valley) was used to delineate

22 BMP configuration units. Four BMPs which are used in actual Chinese red-soil regions (Closing  
23 measures, Arbor-bush-herb mixed plantation, Low-quality forest improvement, and Orchard  
24 improvement) were considered in the proposed approach to achieve the multiple optimization  
25 objectives, which included maximizing the reduction ratio of soil erosion and minimizing the net  
26 cost of the BMP scenario. The proposed approach was compared with the approach which selects  
27 and allocates BMPs randomly on BMP configuration units. The results show that the proposed  
28 approach is more effective and efficient for proposing practical and effective BMP scenarios than  
29 the random approach.

30 **Key words:** best management practices—spatial optimization—slope position units—watershed  
31 process simulation—genetic algorithm

32  
33 **Best Management Practices (BMPs) are a series of management practices that implemented**  
34 **at different spatial scales (e.g., site, field, streambank, and sub-basin) to control soil erosion,**  
35 **reduce nonpoint source pollution, and protect the ecological environment of a watershed**  
36 (Gitau et al. 2004; Turpin et al. 2005; Arabi et al. 2006; Panagopoulos et al. 2012). Spatial  
37 optimization of BMPs based on watershed modeling coupled with intelligent optimization  
38 algorithms (e.g., NSGA- II; Deb et al. 2002) is an effective watershed management planning  
39 approach to proposing optimal BMP scenarios (i.e., selection and allocation of multiple BMPs for  
40 spatial units in watershed) as a balance between consideration of both environmental effectiveness  
41 and cost-benefit (Veith et al. 2004; Duinker and Greig 2007; Maringanti et al. 2011). Watershed  
42 models are used to simulate the watershed response (e.g., flow, sediment, nitrogen, and phosphorus)

43 to each BMP scenario and then evaluate its environmental effectiveness. One of the key elements  
44 that affects how a watershed responds to a BMP scenario is the spatial configuration of its BMPs  
45 on spatial units in the watershed (Heathwaite et al. 2000; Sahu and Gu 2009).

46 The commonly used spatial units for BMP configurations (hereafter called BMPs  
47 configuration units) in existing studies of spatial BMP optimization include sub-basins (Chang et  
48 al. 2007; Chichakly et al. 2013), hydrologic response units (HRUs) (Maringanti et al. 2011), farms  
49 (Gitau et al. 2004), and fields (Srivastava et al. 2003; Kalcic et al. 2015b; Wu et al. 2017). A sub-  
50 basin is normally regarded as a relatively closed and independent spatial unit. A sub-basin consists  
51 of hillslopes which can be further delineated into different homogeneous functional units from the  
52 perspective of physical geography (such as geomorphic, soil, and hydrologic conditions), e.g.,  
53 landform positions (Band 1999). Since individual BMPs are often more effective when applied to  
54 specific homogeneous functional units, the sub-basin unit is too general for spatially-explicit BMP  
55 configurations.

56 HRUs represent hydrologic homogeneous areas combined in terms of landuse, soil, and slope  
57 within one sub-basin (Arnold et al. 1998). One HRU may occupy several parts on a hillslope (e.g.,  
58 separate ridge and valley areas), and HRUs are not internally linked within one sub-basin (Arnold  
59 et al. 2010; Bieger et al. 2016). This characteristic means that the impact of spatial relationships  
60 between BMP configuration units (e.g., the impact of upslope BMPs on downslope units) cannot  
61 be effectively assessed when those units are HRUs (Arnold et al. 2010). Therefore, the HRU is  
62 incapable of being the BMP configuration unit for spatially-explicit BMP configurations,  
63 especially for those BMPs (e.g., conservation management systems) which have different effects

64 on locations with various topographic, landuse, or soil conditions (Heathwaite et al. 2000; Jiang et  
65 al. 2007; Mudgal et al. 2010).

66 Farms and fields are often defined according to land ownership, current landuse, or soil type  
67 boundaries (Srivastava et al. 2003; Gitau et al. 2004; Kalcic et al. 2015a; Wu et al. 2017). A farm  
68 or field may be delineated roughly across multiple landform positions or sub-basins (Srivastava et  
69 al. 2003; Kalcic et al. 2015a; Wu et al. 2017), which results in weak spatial relationships to  
70 homogeneous functional units. Such delineated spatial units face shortcomings similar to those  
71 faced by sub-basins and HRUs. Occasionally, farms or fields are delineated as a patchwork of  
72 gridded cells (even as individual gridded cells; Gaddis et al. 2014) within homogeneous functional  
73 units. This results in a large number of BMP configuration units, which can make the spatial  
74 optimization process computationally intensive or even unsolvable (Gaddis et al. 2014; Wu et al.  
75 2017).

76 Therefore, the spatial units for BMP configurations should be homogeneous functional units  
77 with a comparatively limited count per study area, and currently used BMPs configuration units  
78 are not suitable. In this study, we propose to use slope positions as the spatial units for BMP  
79 configurations. There are two main reasons for this selection: the physical geographic features of  
80 spatial units, and the computational requirements of BMP optimization based on the spatial units.  
81 With respect to the first point, slope positions (also referred as landform positions or landscape  
82 positions) are spatially contiguous and topographically connected units along hillslope (e.g., ridge,  
83 backslope, and valley). Slope positions, which are basic landform units in a hierarchical structure  
84 of spatial units (i.e., slope position, hillslope, sub-basin, and so on), inherently relate to physical

85 watershed processes (Swanson et al. 1988; Band 1999; Qin et al. 2009; Ajami et al. 2016; Bieger  
86 et al. 2016). Slope positions affect various hillslope-scale processes (e.g., surface runoff and soil  
87 erosion, Mudgal et al. 2010) and hence affect both soil hydrologic properties (Jiang et al. 2007;  
88 Qin et al. 2012; Geng et al. 2017) and the effectiveness of BMPs (Bosch et al. 2012; Hernandez-  
89 Santana et al. 2013). Researchers have suggested considering the characteristics of both BMPs and  
90 slope positions during the selection and allocation of BMPs (Berry et al. 2005; Goddard 2005;  
91 Pennock 2005; Mudgal et al. 2010). For example, Cai et al. (2012) empirically summarized the  
92 spatial relationships between BMPs and slope positions based on the characteristics of soil erosion  
93 in the Chinese red-soil region and the practical management experiences of soil and water  
94 conservation in this region. According to the integrated management scheme (figure 1) proposed  
95 by Cai et al. (2012), natural restoration and ecologic forest-grass management schemes are suitable  
96 on the upslope, development management practices such as economical forest-fruit could be  
97 conducted on the midslope, while terrace and riparian buffer strips are proper BMPs for the  
98 downslope. The other reason for considering slope positions as spatial units is that under a specific  
99 system of slope positions, the number of slope positions in a study area is normally limited and  
100 much lower than the count of gridded cells for the area. This can reduce the search space during  
101 spatial optimization and save computing resources. Thus, slope position units should be the proper  
102 spatial units for BMP configuration.

103

104

(Figure 1 is about here.)

105

106 Currently, slope positions have not been used as BMP configuration units for spatial  
107 optimizations of BMPs at the watershed scale, although slope position units have been integrated  
108 into process-based distributed watershed models, such as SWAT+ (Bieger et al. 2016) and SMART  
109 (Soil Moisture And Runoff simulation Toolkit; Ajami et al. 2016). A few studies examined the  
110 effectiveness of BMPs on different slope positions based on watershed modeling by manually  
111 designed BMP scenarios (Sahu and Gu 2009; Mudgal et al. 2010). For example, using SWAT with  
112 a hillslope-discretization scheme, Sahu and Gu (2009) examined the effect of both size (i.e., 10%,  
113 20%, 30%, and 50% of sub-basin area) and spatial location (i.e., the mid-way of the hillslope or  
114 riparian buffer) of filter strips on reducing NO<sub>3</sub>-N in an agricultural watershed. In the study by  
115 Sahu and Gu (2009), the mid-way of the hillslope was defined as a percentage of sub-basin area  
116 instead of a homogeneous functional unit. Thus, this method of BMP allocation is not spatially  
117 explicit. Mudgal et al. (2010) used the APEX model to evaluate the impact of different slope  
118 position sequences (e.g., summit-backslope-footslope, footslope-backslope-summit, and so on)  
119 and the sizes of slope positions on the simulation of runoff and dissolved atrazine load at thirty  
120 designated plots with a size of 189m × 18m. Although the slope position sequences considered in  
121 Mudgal et al. (2010) were theoretical and some of them may not exist naturally (e.g., backslope-  
122 footslope-summit), their results still indicated that taking account of slope positions may be  
123 beneficial when making management decisions.

124 In this study, we examined the effectiveness of using slope positions as BMP configuration  
125 units in the spatial optimization of BMPs for mitigating soil erosion at the watershed scale. The  
126 spatial optimization of watershed BMPs based on slope position units was designed as a

127 methodological framework and then was implemented in a case study area by following tasks: (1)  
128 delineating slope position units from gridded DEM of the study area; (2) spatially distributed  
129 watershed modeling for simulating watershed processes related to soil erosion in the study area,  
130 which was used to evaluate the environmental effectiveness of each BMPs scenario; (3) developing  
131 a knowledge base of BMPs considered in the study area which contains the spatial relationships  
132 between BMPs and slope positions; and (4) adopting a multi-objective optimization method to  
133 apply the BMP knowledge base to optimizing BMP scenarios based on slope position units. The  
134 optimization results of the proposed approach were compared with those from the standard random  
135 optimization approach which selects and allocates BMPs randomly to configuration units.

## 136 **Materials and Methods**

137 *Methodology.* To use slope positions as BMP configuration units during spatial optimization of  
138 BMPs at the watershed scale, the design of such a new approach should deal with three key issues,  
139 which are different from those in currently-used approach. The first is how to delineate slope  
140 positions for an area. There are several methods of delineating slope positions by digital terrain  
141 analysis on digital elevation models (DEM) in a manner of either crisp or fuzzy classification (e.g.,  
142 Pennock et al. 1987; Schmidt and Hewitt 2004; Qin et al. 2009; Miller and Schaetzl 2015).

143 The second is to formalize the knowledge of the spatial relationships between BMPs and  
144 slope positions, which can be stored together with other BMP knowledge in a BMP knowledge  
145 base and then applied to the multi-objective optimization process. The spatial relationships  
146 between BMPs and slope positions can be summarized as two main types: the suitable BMPs for  
147 each type of slope position, and the spatial constraint among BMPs on different types of slope

148 position (normally along the hillslope from upstream to downstream; e.g., if a BMP is placed in a  
149 downslope unit, there is no need to place BMPs in its adjacent upslope units (Wu et al. 2017)).  
150 This knowledge of the spatial relationships between BMPs and slope positions can be formalized  
151 as rules and stored in the BMP knowledge base.

152 The third is how to combine the formalized knowledge of the spatial relationships between  
153 BMPs and slope positions with intelligent optimization algorithms. Note that intelligent  
154 optimization algorithms applied to spatial BMP optimization normally initialize and generate BMP  
155 scenarios through selecting and allocating BMPs randomly to spatial configuration units. When  
156 knowledge of the spatial relationships between BMPs and slope positions is available in the form  
157 of rules, those BMP scenarios generated and evaluated by intelligent optimization algorithms will  
158 be constrained by this knowledge. Thus, many unreasonable BMP scenarios will not be considered  
159 in the multi-objective optimization process, which results in greater optimization efficiency. In  
160 addition, the optimal BMP scenarios resulting from such a process are more likely to be reasonable  
161 and practical.

162 Based on the ideas presented above, the framework for the spatial optimization of watershed  
163 BMPs based on slope position units proposed in this study is shown in figure 2. The following  
164 parts of this section will describe the implementation of the proposed methodological framework  
165 in a case study area.

166  
167 (Figure 2 is about here.)

168

169 **Study area.** The Youwuzhen watershed (~5.39 km<sup>2</sup>), which is a part of Zhuxi watershed within  
170 Changting county of Fujian province, was chosen as the study area (figure 3). The study area is  
171 located in the typical red-soil hilly region in southeastern China and suffers from severe soil  
172 erosion (Chen et al. 2013). Its primary geomorphological characteristics include low hills with  
173 steep slopes (up to 52.9° and with an average slope of 16.8°) and broad alluvial valleys. The  
174 elevation ranges from 295.0 m to 556.5 m. The study area is under a mid-subtropical monsoon  
175 moist climate. The annual average temperature is 18.3 °C. The annual average precipitation is  
176 1697.0 mm, while intense short-duration thunderstorm events contribute about three quarters of  
177 annual precipitation from March to August (Chen et al. 2013). The main landuse types are forest,  
178 paddy field, and orchard, with an area ratio of 59.8%, 20.6%, and 12.8%, respectively. Forests in  
179 the study area are mostly secondary or human-made forests with scattered Masson's pine (*Pinus*  
180 *massoniana*) (Chen et al. 2013; Chen et al. 2017). Soil types in the study area are dominated by  
181 red earth (Humic Acrisols in FAO soil taxonomy, or Ultisols in US soil taxonomy) which was  
182 highly weathered from granite and inherently infertile, acidic, nutrient-deficient, poor in organic  
183 matter, and low capacity for holding and supplying water (He et al. 2004; Chen et al. 2013).

184

185 (Figure 3 is about here.)

186

187 **Delineation of slope position units.** Without loss of generality, this study uses a simple system of  
188 three types of slope positions (i.e., ridge, backslope, and valley), which has been applied in existing  
189 watershed modeling (e.g., Arnold et al. 2010; Ajami et al. 2016). In addition, a hierarchical

190 structure of spatial units, i.e., sub-basin, hillslope, and slope position, is maintained, so as to  
191 support the representation of the spatial relationships between BMPs and slope positions along a  
192 hillslope in the spatial BMP optimization.

193 A gridded DEM with 10 m resolution of the Youwuzhen watershed was created from a  
194 1:10,000 topographical map with a contour interval of 5 m by the “Topo To Raster” tool of ArcGIS  
195 10.3 software. Sub-basins were delineated based on an accumulated threshold of 0.185 km<sup>2</sup> (Chen  
196 et al. 2013). For each sub-basin, which consists of headwater, left hillslope, and right hillslope  
197 (relative to flow direction), hillslopes were then delineated according to the D8 flow direction  
198 model (O’Callaghan and Mark 1984). Each hillslope contains slope position units with  
199 downstream and upstream relationships.

200 A prototype-based inference method proposed by Qin et al. (2009) was adopted to derive the  
201 fuzzy memberships of each cell to the three slope positions. This method was chosen because it  
202 can reasonably perform fuzzy inference on both attribute and spatial domains. Then, a crisp  
203 classification map of slope position units in the study area was obtained by a “hardening” process,  
204 i.e., applying the maximum membership principle cell-by-cell to all fuzzy membership maps of  
205 individual slope position types resulting from the prototype-based inference method (Qin et al.  
206 2009).

207 The numbers of sub-basin, hillslope, and slope position units delineated in the study area are  
208 17, 35, and 105, respectively (figure 4).

209

210

(Figure 4 is about here.)

211  
212 ***Watershed processes modeling and calibration.*** SEIMS (Spatially Explicit Integrated Modeling  
213 System), a spatially explicit watershed modeling framework whose original hydrologic model is  
214 WetSpa (Water and Energy Transfer between Soil, plant, and atmosphere) (Liu et al. 2003; Liu  
215 2004), was selected because of its spatially-explicit representation of watershed processes and  
216 flexible modular framework for coupling various watershed processes modules and scenario  
217 analysis (Liu et al. 2014, 2016). SEIMS has been extended to simulate long-term watershed  
218 processes including hydrology, soil erosion, and plant growth. The representation of BMPs in  
219 SEIMS is implemented through the relative alterations of model parameters which characterize  
220 BMPs environmental effects in the locations of BMPs placement (Wu et al. 2017). SEIMS is still  
221 under continuous development and the source code is available on Github  
222 (<https://github.com/lreis2415/SEIMS>).

223 The hydrologic processes simulated in this study include interception, surface depressional  
224 storage, surface runoff, infiltration, potential evapotranspiration, percolation, interflow,  
225 groundwater flow, and channel flow. The interception process is simulated by the maximum  
226 canopy storage method proposed by Aston (1979). The depression storage is estimated by an  
227 empirical equation suggested by Linsley et al. (1975). Surface runoff and infiltration are estimated  
228 using a modified coefficient method which depends on slope, land use, soil type, soil moisture,  
229 and rainfall intensity, etc. (Liu 2004). The potential evapotranspiration is estimated by Priestley-  
230 Taylor equation (Priestley and Taylor 1972). The percolation process is simulated using the method  
231 in SWAT when the water content of the soil layer exceeds the field capacity and the layer below it

232 is not saturated (Neitsch et al. 2011). Interflow (or shallow subsurface lateral flow) is assumed to  
233 occur after percolation and cease when soil moisture is lower than field capacity and is simulated  
234 from Darcy's Law and the kinematic approximation (Liu 2004). The groundwater flow is estimated  
235 with a linear reservoir method as a function of groundwater storage and a recession coefficient on  
236 sub-basin scale (Liu 2004). The overland flow routing algorithm is adapted from a diffusive  
237 transport approach proposed by Liu et al. (2003). The Muskingum method (Cunge 1969) is used  
238 for channel flow routing.

239 Sediment yield caused by water erosion is estimated for each cell with the Modified Universal  
240 Soil Loss Equation (MUSLE) (Williams 1975) at each cell and is routed into channels with surface  
241 runoff. A simplified Bagnold stream power equation from Williams (1980) is used for sediment  
242 routing in stream channels, in which the maximum amount of sediment that can be transported  
243 from a reach segment is a function of the peak channel velocity (Neitsch et al. 2011).

244 Plant growth process in SEIMS is adapted from SWAT model, which is a simplified version  
245 of EPIC plant growth model (Williams 1995) and utilizes a single plant growth model to simulate  
246 all types of land covers.

247 The data necessary for watershed modeling and calibration based on SEIMS (i.e., the spatial  
248 data such as DEM, soil, landuse, and climate data, and site-monitoring data at the watershed outlet)  
249 were collected. The landuse map was manually interpreted from ALOS image derived in 2009  
250 (Chen et al. 2013). The soil type map was from the Second National Soil Survey of Changting  
251 county with a scale of 1:50,000 (Chen et al. 2013). Soil properties such as mechanical composition  
252 and organic matter were measured from field samplings (Chen et al. 2013; Xie et al. 2015). Other

253 soil water characteristics (e.g., soil hydraulic conductivity, and field capacity) were calculated with  
 254 the SPAW model (Saxton and Rawls 2006). Soil erodibility factors, cover management factors,  
 255 and conservation practice factors for the USLE model were drawn from the study in this area by  
 256 Chen and Zha (2016). Daily meteorological data and precipitation were derived from National  
 257 Meteorological Information Center of China Meteorological Administration data and the local  
 258 monitoring station, respectively. The periodic monitoring flow and sediment discharge data at the  
 259 watershed outlet from 2013 to 2015 were provided by the Soil and Water Conservation Bureau of  
 260 Changting county, Fujian province, China.

261 To calibrate the watershed model for the following spatial optimization of BMPs, we selected  
 262 those periods with available data and rainstorms which had more than three consecutive days of  
 263 rainfall and for which there are complete records of runoff generation and sediment yield. As a  
 264 result, the years of 2013 and 2014 were selected for watershed model calibration, and the year of  
 265 2015 was selected for validation of the watershed model.

266 Model performance indicators such as *NSE* (equation 1), *PBIAS* (equation 2), and *RSR*  
 267 (equation 3) recommended by Moriasi et al. (2007) were used to evaluate the watershed model.

$$268 \quad NSE = 1 - \frac{\sum_{i=1}^n (Y_i^{obs} - Y_i^{sim})^2}{\sum_{i=1}^n (Y_i^{obs} - Y^{mean})^2} \quad (1)$$

$$269 \quad PBIAS = \frac{\sum_{i=1}^n (Y_i^{obs} - Y_i^{sim}) * 100}{\sum_{i=1}^n Y_i^{obs}} \quad (2)$$

270

$$RSR = \frac{\sqrt{\sum_{i=1}^n (Y_i^{obs} - Y_i^{sim})^2}}{\sqrt{\sum_{i=1}^n (Y_i^{obs} - Y^{mean})^2}} \quad (3)$$

271 where  $Y_i^{obs}$  and  $Y_i^{sim}$  are the  $i$ th observed and simulated values, respectively;  $Y^{mean}$  is the average  
 272 of all observed values;  $n$  is the number of observed values.

273 The modeling performance of the manually calibrated SEIMS model for flow discharge and  
 274 sediment export, both in the calibration and validation periods, are shown in figures 5 and 6,  
 275 respectively. The calibration of flow has an  $NSE$ ,  $RSR$ ,  $PBIAS$ , and  $R^2$  of 0.48, 0.72, -16.24%, and  
 276 0.58, respectively (figure 5a). According to the general performance ratings for simulations at a  
 277 monthly time step by Moriasi et al. (2007), the model performance is satisfactory when the model  
 278 results receive a value of  $NSE$ ,  $RSR$ , and  $PBIAS$  better than 0.50, 0.60, and  $\pm 25\%$  (for sediment it  
 279 is  $\pm 55\%$ ), respectively. Thus, the performance of flow is approximately satisfactory. For sediment,  
 280 the  $NSE$ ,  $RSR$ ,  $PBIAS$ , and  $R^2$  are 0.31, 0.83, -40.55%, and 0.36, respectively (figure 6a). Although  
 281 the overall simulated trend is consistent with the observed values according to  $R^2$ , the simulation  
 282 results still overestimated the low values and underestimated the peak sediment exports (figure 6a).  
 283 This is similar to other cases in which model simulations are generally poorer for shorter time  
 284 steps than for longer time steps (Engel et al. 2007). The performance of sediment can be regarded  
 285 as acceptable.

286  
 287 (Figure 5 is about here.)

288 (Figure 6 is about here.)

289

290 Although the performance statistics for the validation period are poor for flow and sediment  
291 (figure 5b and figure 6b), the general trends of hydrographs in the study area can still be captured  
292 by the calibrated SEIMS model from a visual perspective. This means the calibrated model can be  
293 used for the following spatial optimization of BMPs. Therefore, the year of 2013 was used as  
294 simulation period and the scenario for model calibration was selected as the baseline scenario. The  
295 BMP scenarios generated during the spatial optimization will be evaluated for 2013 by the  
296 calibrated SEIMS model.

297 ***BMPs knowledge base.*** Four BMPs that have been implemented in Changting county for soil and  
298 water conservation are considered in this study: Closing measures (CM), Arbor-bush-herb mixed  
299 plantation (ABHMP), Low-quality forest improvement (LQFI), and Orchard improvement (OI).  
300 Their brief descriptions are listed in table 1 (Chen et al. 2013; Chen et al. 2017).

301

302 (Table 1 is about here.)

303

304 The BMP knowledge base for this study mainly includes three components: the cost-benefit,  
305 the environmental effects, and the spatial relationships between BMPs and slope positions. The  
306 first two components are normal components in BMP knowledge bases for existing approaches to  
307 spatial BMP optimization, while the third is specific to the proposed approach.

308 The cost-benefit for each BMP consists of initial implementation cost, annual maintenance  
309 cost, and annual benefit estimated from local government project (table 2; Wang 2008).

310

311 (Table 2 is about here.)

312

313 For evaluating the environmental effects of BMPs on mitigating soil erosion, the relative  
314 improvements of major parameters related to hydrologic and soil erosion processes were collected  
315 and are listed in table 3. Relative changes to the conservation practice factors in the USLE model  
316 (i.e., USLE\_P) in table 3 were adopted from the calibrated SWAT model in Chen et al. (2013).  
317 Other factors were calculated directly (e.g., organic matter, bulk density, and total porosity) or  
318 indirectly (e.g., soil hydraulic conductivity and soil erodibility factor of USLE model) from the  
319 sample-plot data provided by Fujian Soil and Water Conservation Monitoring Station et al. (2010).  
320 These sample-plot locations were collected from locations where their respective BMPs have been  
321 implemented for 8 years, and they were compared with control groups retaining their original  
322 landuses without the implementation of BMPs.

323

324 (Table 3 is about here.)

325

326 As stated above, the knowledge of the spatial relationships between the four BMPs and slope  
327 positions were formalized as two types of rules for the study area. Rules of the first type, i.e., the  
328 suitable BMPs for each type of slope position, are generalized from the description in table 1 and  
329 formalized in table 4. Rules of the second type, i.e., the spatial constraint among BMPs on different  
330 types of slope position along the hillslope from upstream to downstream, are based on an  
331 effectiveness grade which represents the degree of improvement in the area of mitigating soil  
332 erosion (table 4). The effectiveness grades range from 1 to 5, with higher-numbered grades

333 representing better effectiveness. In the current study, a simple rule is adopted according to local  
334 experience (Chen et al. 2013), i.e., the effectiveness grade of the BMP placed on the backslope of  
335 a hillslope should be greater than or equal to that of the BMP placed on the ridge of the same  
336 hillslope. For example, the effectiveness order of BMP sequences for ridge and backslope of a  
337 hillslope should be ABHMP-ABHMP > CM-ABHMP > CM-CM, while the solution of ABHMP-  
338 CM will be ignored because the effectiveness grade of CM (i.e., 3) is less than that of ABHMP  
339 (i.e., 5).

340

341

(Table 4 is about here.)

342

343 ***Multi-objective optimization by intelligent optimization algorithm.*** The Non-dominated Sorted  
344 Genetic Algorithm (NSGA-II) (Deb et al. 2002) was selected as the intelligent optimization  
345 algorithm for the proposed approach. NSGA-II can ensure that the optimization solutions are  
346 diverse and well distributed in all objective functions under consideration according to its non-  
347 dominated sorting and elitism properties (Zitzler and Thiele 1999). NSGA-II has been widely  
348 applied to spatial BMP optimization with multi-objectives (e.g., maximum environmental  
349 effectiveness and minimum net cost) (Rodriguez et al. 2011; Panagopoulos et al. 2012; Yang and  
350 Best 2015).

351 When the NSGA-II is applied to spatial BMP optimization, an individual of a population  
352 corresponds to a BMP scenario and is represented as a chromosome with genes as variables (i.e.,  
353 BMP configuration units with selected BMP type or without BMP). The execution of NSGA-II

354 includes an initialization process of initializing a population of individuals and then a circular  
355 process of evaluation and generation of BMP scenarios. For each round (or, equivalently,  
356 generation) of the process, the fitness of each individual in the current population is evaluated by  
357 objective functions (e.g., environmental effectiveness based on the calibrated watershed model,  
358 and economic benefit calculation by BMPs cost model). In the following selection process, the  
359 fittest individuals are selected (i.e., duplicated for next round) and those weak individuals are  
360 discarded from the population. Those selected individuals are stored as an elite set which is known  
361 as near Pareto optimal solutions (Deb et al. 2002) and will be updated by successive generations.  
362 The offspring are generated by crossover and mutation operators (or, equivalently, regeneration),  
363 and then are added to the population for next round of evaluation. This process is repeated until a  
364 given maximum generation number has been reached.

365       When the NSGA- II is adopted by the proposed approach to spatial BMP optimization, the  
366 spatial relationships between BMPs and slope positions along the hillslopes are incorporated into  
367 the initialization and regeneration (i.e., crossover and mutation) of BMP scenarios. In the  
368 initialization process, the valley unit of each hillslope is first randomly allocated one suitable BMP  
369 or left without a BMP. Then, an iteration procedure is performed to select and allocate BMPs for  
370 other slope position units in an upstream-downstream order (i.e., backslope and ridge by sequence)  
371 based on the rules of spatial relationships between BMPs and slope positions along the hillslope.  
372 In the regeneration process, every BMP scenario generated after crossover and mutation operations  
373 is adjusted according to the rules of spatial relationships between BMPs and slope positions. In  
374 such a way, every BMP scenario evaluated in the spatial BMP optimization is reasonable in terms

375 of the spatial relationships between BMPs and slope positions, which means that the same will be  
 376 true of every optimal BMP scenario. Unreasonable BMP scenarios will not be considered, which  
 377 results in higher optimization efficiency.

378 The multi-objectives in this study are maximizing the reduction rate of soil erosion and  
 379 minimizing the net cost of BMPs (equation 4). The calibrated SEIMS model for the Youwuzhen  
 380 watershed is used to evaluate the reduction rate of soil erosion from each BMP scenario in  
 381 comparison to a baseline scenario (equation 5). A simple BMP cost model (equation 6) is used to  
 382 calculate the net cost of each BMP scenario according to the cost-benefit knowledge in the BMP  
 383 knowledge base.

$$384 \quad \min [(f(X)) \wedge (-g(X))] \quad (4)$$

385 where  $X$  represents a BMP scenario;  $f(X)$  is the reduction rate of soil erosion under  $X$  compared to  
 386 that under the baseline scenario (equation 5); and  $g(X)$  is the net cost of  $X$  (equation 6).

$$387 \quad f(X) = \frac{v(0) - v(X)}{v(0)} \quad (5)$$

$$388 \quad g(X) = \sum_{i=1}^n A(x_i) \times \{ [C(x_i) + yr \times (M(x_i) - B(x_i))] \} \quad (6)$$

389 where  $v(0)$  and  $v(X)$  are the total amounts of soil erosion (kg) under baseline scenario and the  $X$   
 390 scenario, respectively;  $n$  is the number of BMP configuration units (slope position units);  $A(x_i)$  is  
 391 the area covered by the BMP implemented in the  $i$ th configuration unit;  $yr$  is the years since the  
 392 BMP was implemented, which is 8 in this study (see table 3); and  $C(x_i)$ ,  $M(x_i)$ , and  $B(x_i)$  are unit  
 393 costs for initial implementation, annual maintenance, and annual benefit (see table 2), respectively.

394 ***Experimental design.*** The effectiveness of the proposed approach was compared with the

395 traditional approach to spatial BMP optimization (hereafter referred as the random approach)  
396 which initializes and generates individuals by selecting and allocating BMPs on genes  
397 (corresponding to BMP configuration units, i.e., slope position units in this study) randomly.

398 The proposed approach and the random approach were implemented based on a Python  
399 framework for evolutionary computation known as DEAP (Fortin et al. 2012). SCOOP (Hold-  
400 Geoffroy et al. 2014) was incorporated to improve computation efficiency by distributing tasks  
401 dynamically across Linux cluster. Thus, the experiment was conducted on a Linux cluster which  
402 consists of one management node and four computation nodes. Each node has two Intel® Xeon  
403 E5645 CPUs and each CPU has six cores.

404 In the evaluation experiment, the main parameter settings of NSGA- II are the same for both  
405 approaches. The initial population size is 60 with a selection rate of 0.8 and a maximum generation  
406 number of 100. The crossover probability and the mutation probability are 0.75 and 0.15,  
407 respectively.

408 The proposed approach was evaluated with respect to two aspects, i.e., the quality of near  
409 Pareto optimal solutions and the computational efficiency. The quality of near Pareto optimal  
410 solutions was evaluated via three methods. The first is visual interpretation of the convergence and  
411 diversity of near Pareto optimal solutions derived from all generations. The second is based on the  
412 hypervolume index (Zitzler and Thiele 1999), which measures the volume (area for two-  
413 dimensions) of objective space covered by a set of near Pareto optimal solutions. A higher  
414 hypervolume index indicates a better quality of solutions. The change of the hypervolume index  
415 with generations can provide a quantitative comparison of the quality of near Pareto optimal

416 solutions considering both convergence and diversity (Zitzler et al. 2003). In this study, the  
417 reference point for calculating the hypervolume index is (300, -1) which represents the economic  
418 benefit being 300 million RMBY and the reduction rate of soil erosion being -1. Note that both the  
419 hypervolume index and near Pareto optimal front represent evaluations from a mathematical  
420 perspective and have less practical meaning than the spatial configuration of BMP scenarios when  
421 it comes to decision-making for watershed management. Therefore, the third method is to discuss  
422 the rationality of the spatial configurations of examples selected from the near Pareto optimal  
423 solutions.

## 424 **Results and Discussion**

425 *Near Pareto optimal solutions derived from all generations.* Figure 7 shows the near Pareto  
426 optimal solutions derived from all generations by the proposed approach and the random approach.  
427 From the visual interpretation, the proposed approach shows a better convergence and a similar  
428 diversity in the Pareto optimal front, compared to the random approach (figure 7). During the  
429 spatial optimization, the calibrated SEIMS model for the Youwuzhen watershed was executed to  
430 evaluate 1476 BMP scenarios for the proposed approach and 1523 BMP scenarios for the random  
431 approach, while the total runtimes were 8.7 and 11.8 hours, respectively. This means that with the  
432 constraint of the relationships between BMPs and slope positions, the proposed approach can  
433 reduce the search space of optimal solutions, and hence improve the computational efficiency  
434 (Maier et al. 2014).

435

436

(Figure 7 is about here.)

437  
438 ***The change of hypervolume index with generations.*** The change of the hypervolume index with  
439 generations (figure 8) shows that the proposed approach has an obvious advantage over the random  
440 approach when the generation number is less than 35, especially in the first 10 generations (e.g.,  
441 figure 9a and figure 9b). With the increase of generation number, the hypervolume index values  
442 from the two approaches are similar until the random approach produced steadily higher values of  
443 the hypervolume index after the 65<sup>th</sup> generation.

444 This effect might be a result of the fact that the search space for the proposed approach is  
445 constrained by the BMP knowledge base, and thus is a subset of the search space for the random  
446 approach. Therefore, the proposed approach can lead individuals (i.e., BMP scenarios) to the ideal  
447 Pareto optimal front more rapidly than the random approach at the early phase of optimization  
448 (e.g., figure 9a and figure 9b). This result also suggested that it can be effective to utilize the rules  
449 of spatial relationships between BMPs and slope positions as a priori knowledge to achieve better  
450 solutions during optimization (Bi et al. 2015; Wu et al. 2017). In the late phase of the optimization,  
451 the random approach can generate scenarios beyond the search space of the proposed approach  
452 and could reach a higher hypervolume index value (e.g., figure 8 and figure 9d). This phenomenon  
453 is common in similar comparison studies, such as Pyo et al. (2017). Although this means a better  
454 set of near Pareto optimal solutions from the mathematical perspective, the scenarios in this set  
455 might not be practical in terms of their spatial configurations of BMPs, as discussed in the  
456 following section.

457

458 (Figure 8 is about here.)

459 (Figure 9 is about here.)

460

461 ***Spatial configuration of selected BMP scenarios.*** BMP scenarios from each approach with similar  
462 economic effectiveness (i.e., 0.5 million RMBY net cost) were randomly selected from the near  
463 Pareto optimal solutions of the 10<sup>th</sup> generation (figure 9b) and mapped as figure 10. The BMP  
464 scenario from the proposed approach could achieve a 32.4% reduction rate of soil erosion while  
465 that from the random approach could achieve 21.2%. In the BMP scenario shown in figure 10a,  
466 the BMPs allocated by the proposed approach are mainly Closing Measures (CM) and Arbor-bush-  
467 herb mixed plantation (ABHMP), and are distributed mainly on ridges and backslopes. This  
468 matches the relationships between BMPs and slope positions. However, in the BMP scenario from  
469 the random approach (figure 10b), there are several inappropriate allocations violating the  
470 relationships between BMPs and slope positions, e.g., allocating Orchard improvement (OI) on  
471 ridges and Closing measures (CM) on valleys. These inappropriate allocations make this BMP  
472 scenario unreasonable for practical engineering. Thus, in the 10<sup>th</sup> generation at the early phase of  
473 optimization, the proposed approach can derive more practicable and effective optimal BMP  
474 scenarios than the random approach.

475

476 (Figure 10 is about here.)

477

478 Another two BMP scenarios from the proposed approach and the random approach with  
479 similar environmental effectiveness (i.e., 48% reduction rate of soil erosion) were randomly

480 selected from the near Pareto optimal solutions of the 100<sup>th</sup> generation (figure 9d) and mapped in  
481 figure 11. The net cost of the scenario from the proposed approach (i.e., 1.22 million; figure 11a)  
482 would be higher than the cost of the scenario from the random approach (i.e., 1.15 million; figure  
483 11b). From the mathematical view, the random method generates a more optimal solution than the  
484 proposed approach. However, the spatial BMP configuration of the scenario from the random  
485 approach still shows several inappropriate allocations which violate the relationships between  
486 BMPs and slope positions, which means that it is impractical for watershed management.

487

488

(Figure 11 is about here.)

489

## 490 **Conclusion**

491 This paper proposes a spatial optimization approach to watershed BMPs based on slope  
492 position units. In the proposed approach, slope position units, as homogeneous spatial units with  
493 physical geographic features, are used as BMP configuration units by which the spatial  
494 relationships between BMPs and slope positions can be explicitly considered in spatial BMP  
495 optimization.

496 The proposed approach combined with a spatially distributed and physically-based watershed  
497 model (i.e., SEIMS) and a genetic algorithm (i.e., NSGA- II) was applied to a small watershed for  
498 spatial BMP optimization with the multi-objectives of maximizing the reduction ratio of soil  
499 erosion and minimizing the net cost of the BMP scenario. Experimental results show that the  
500 proposed approach is effective and efficient at proposing practicable BMP scenarios for integrated

501 watershed management, when compared to the random approach.

502 The proposed spatial optimization approach to watershed BMPs based on slope position units  
503 can be easily combined with other watershed models (e.g., SWAT+; Bieger et al. 2016), intelligent  
504 optimization algorithms (e.g., SPEA2; Zitzler et al. 2001), slope positions systems (e.g., five slope  
505 positions used in Qin et al. (2009)), and other BMPs available for different study areas.

506 This study also raises several study issues for future work: 1) comparison with the adoption  
507 of other spatial BMP configuration units; 2) improvement of the intelligent optimization algorithm  
508 to accelerate the evolution of Pareto optimal solutions, especially for large watersheds with high  
509 numbers of slope position units and many BMPs under consideration.

510

## 511 **Acknowledgements**

512 This study was funded by the National Key Technology R&D Program (No.  
513 2013BAC08B03-4), the Natural Science Foundation of China (No. 41422109, 41431177), and the  
514 Innovation Project of LREIS (No. O88RA20CYA).

515

## 516 **References**

517 Ajami, H., U. Khan, N. K. Tuteja, and A. Sharma. 2016. Development of a computationally  
518 efficient semi-distributed hydrologic modeling application for soil moisture, lateral flow and  
519 runoff simulation. *Environmental Modelling & Software* 85 (November):319-331.  
520 Arabi, M., R.S. Govindaraju, M.M. Hantush, and B.A. Engel. 2006. Role of watershed subdivision

521 on modeling the effectiveness of best management practices with SWAT. Journal of the  
522 American Water Resources Association (JAWRA) 42(2):513-528.

523 Arnold, J.G., P.M. Allen, M. Volk, J.R. Williams, and D.D. Bosch. 2010. Assessment of different  
524 representations of spatial variability on SWAT model performance. Transactions of the  
525 ASABE 53(5):1433-1443.

526 Arnold, J.G., R. Srinivasan, R.S. Muttiah, and J.R. Williams. 1998. Large area hydrologic  
527 modeling and assessment Part I: Model development. Journal of the American Water  
528 Resources Association (JAWRA) 34(1):73-89.

529 Aston, A. 1979. Rainfall interception by eight small trees. Journal of Hydrology 42(3):383-396.

530 Band, L. 1999. Spatial hydrography and landforms. *In* GIS: Management issues and applications,  
531 edited by P. Longley, M. Goodchild, D. Maguire, and D. Rhind, 527-542. John Wiley & Sons.

532 Berry, J.K., J.A. Delgado, F.J. Pierce, and R. Khosla. 2005. Applying spatial analysis for precision  
533 conservation across the landscape. Journal of Soil and Water Conservation 60(6):363-370.

534 Bi, W., G. C. Dandy, and H. R. Maier. 2015. Improved genetic algorithm optimization of water  
535 distribution system design by incorporating domain knowledge. Environmental Modelling &  
536 Software 69 (July):370-381.

537 Bieger, K., J.G. Arnold, H. Rathjens, M.J. White, D.D. Bosch, P.M. Allen, M. Volk, and R.  
538 Srinivasan. 2016. Introduction to SWAT+, a completely restructured version of the soil and  
539 water assessment tool. Journal of the American Water Resources Association (JAWRA)  
540 53(1):115-130.

541 Bingner, R.L., F.D. Theurer, Y.P. Yuan. 2015. AnnAGNPS technical processes: documentation

542 Version5.4.

543 [https://www.wcc.nrcs.usda.gov/ftpref/wntsc/H&H/AGNPS/downloads/AnnAGNPS\\_Techni](https://www.wcc.nrcs.usda.gov/ftpref/wntsc/H&H/AGNPS/downloads/AnnAGNPS_Techni)

544 [cal\\_Documentation.pdf](#)

545 Bosch, D. D., C. C. Truman, T. L. Potter, L. T. West, T. C. Strickland, and R. K. Hubbard. 2012.

546 Tillage and slope position impact on field-scale hydrologic processes in the South Atlantic

547 Coastal Plain. *Agricultural Water Management* 111(August):40-52.

548 Cai, Q.G., A.X. Zhu, H.X. Bi, L.Y. Sun. 2012. Paradigms for integrated soil and water conservation

549 over main water erosions in China. Beijing: China Water Power Press. (in Chinese)

550 Chang, C.L., P.T. Chiueh, and S.L. Lo. 2007. Effect of spatial variability of storm on the optimal

551 placement of best management practices (BMPs). *Environmental Monitoring and*

552 *Assessment* 135(December):383-389.

553 Chen, S. F., and X. Zha. 2016. Evaluation of soil erosion vulnerability in the Zhuxi watershed,

554 Fujian Province, China. *Natural Hazards* 82(3):1589-1607.

555 Chen, Z.B., Z.Q. Chen, H Yue. 2013. Comprehensive research on soil and water conservation in

556 granite red soil region: A case study of Zhuxi watershed, Changting county, Fujian province.

557 Beijing, Science Press. (in Chinese)

558 Chen, Z.Q., Z.B. Chen, L.Y. Bai, and Y. Zeng. 2017. A Catastrophe model to assess soil restoration

559 under ecological restoration in the red soil hilly region of China. *Pedosphere* 27(4): 778-787.

560 Chichakly, K.J., W.B. Bowden, and M.J. Eppstein. 2013. Minimization of cost, sediment load, and

561 sensitivity to climate change in a watershed management application. *Environmental*

562 *Modelling & Software* 50(December):158-168.

563 Cunge, J. A. 1969. On the subject of a flood propagation computation method (Muskingum  
564 method). *Journal of Hydraulic Research* 7(2):205-230.

565 Deb, K., A. Pratap, S. Agarwal, and T. Meyarivan. 2002. A fast and elitist multiobjective genetic  
566 algorithm: NSGA- II. *IEEE Transactions on Evolutionary Computation* 6(2):182-197.

567 Duinker, P.N., and L.A. Greig. 2007. Scenario analysis in environmental impact assessment:  
568 improving explorations of the future. *Environmental Impact Assessment Review* 27(3):206-  
569 219.

570 Engel, B., D. Storm, M. White, J. Arnold, and M. Arabi. 2007. A Hydrologic/Water Quality Model  
571 Application. *Journal of the American Water Resources Association (JAWRA)* 43(5):1223-  
572 1236.

573 Fonseca, C. M., L. Paquete, and M. López-Ibáñez. 2006. An improved dimension-sweep algorithm  
574 for the hypervolume indicator. Paper presented at the 2006 IEEE Congress on Evolutionary  
575 Computation, Vancouver, BC, Canada, July 16-21, 2006.

576 Fortin, F.-A., F.-M.D. Rainville, M.-A. Gardner, M. Parizeau, and C. Gagné. 2012. DEAP:  
577 Evolutionary algorithms made easy. *Journal of Machine Learning Research* 13(July):2171-  
578 2175.

579 Fujian Soil and Water Conservation Monitoring Station, Fujian Agriculture and Forestry  
580 University, Fujian Normal University, and Changting Soil and Water Conservation  
581 Monitoring Station. 2010. Monitoring report of soil and water loss in Changting county.  
582 Fuzhou, Fujian, China. (in Chinese)

583 Gaddis, E.J.B., A. Voinov, R. Seppelt, and D.M. Rizzo. 2014. Spatial optimization of best

584 management practices to attain water quality targets. *Water Resources Management*  
585 28(6):1485-1499.

586 Geng, R., G.H. Zhang, Q.H. Ma, and H. Wang. 2017. Effects of landscape positions on soil  
587 resistance to rill erosion in a small catchment on the Loess Plateau. *Biosystems Engineering*  
588 160(August):95-108.

589 Gitau, M.W., T.L. Veith, and W.J. Gburek. 2004. Farm-level optimization of BMP placement for  
590 cost-effective pollution reduction. *Transactions of the ASAE* 47(6):1923-1931.

591 Goddard, T.W. 2005. An overview of precision conservation in Canada. *Journal of Soil and Water*  
592 *Conservation* 60(6):456-461.

593 Heathwaite, L., A. Sharpley, and W. Gburek. 2000. A conceptual approach for integrating  
594 phosphorus and nitrogen management at watershed scales. *Journal of Environmental Quality*  
595 29(1):158-166.

596 He, Z.L., M.K. Zhang, and M.J. Wilson. 2004. Distribution and classification of red soils in China.  
597 *In The Red Soils of China: Their nature, management and utilization*, edited by M.J. Wilson,  
598 Z.L. He, and X.E. Yang, 29-33. Kluwer Academic Publishers.

599 Hernandez-Santana, V., X. Zhou, M. J. Helmers, H. Asbjornsen, R. Kolka, and M. Tomer. 2013.  
600 Native prairie filter strips reduce runoff from hillslopes under annual row-crop systems in  
601 Iowa, USA. *Journal of Hydrology* 477(January):94-103.

602 Hold-Geoffroy, Y., O. Gagnon, and M. Parizeau. 2014. Once You SCOOP, no need to fork. *In*  
603 *Proceedings of the XSEDE'14 Annual Conference on Extreme Science and Engineering*  
604 *Discovery Environment*, Atlanta, GA, July 13-18, 2014. New York, NY: ACM.

605 Jiang, P., S.H. Anderson, N.R. Kitchen, E.J. Sadler, and K.A. Sudduth. 2007. Landscape and  
606 conservation management effects on hydraulic properties of a claypan-soil toposequence.  
607 Soil Science Society of America Journal 71(3):803-811.

608 Kalcic, M.M., I. Chaubey, and J. Frankenberger. 2015a. Defining Soil and Water Assessment Tool  
609 (SWAT) hydrologic response units (HRUs) by field boundaries. International Journal of  
610 Agricultural and Biological Engineering 8(3):69-80.

611 Kalcic, M.M., J. Frankenberger, and I. Chaubey. 2015b. Spatial optimization of six conservation  
612 practices using SWAT in tile-drained agricultural watersheds. Journal of the American Water  
613 Resources Association (JAWRA) 51(4):956-972.

614 Linsley, R. K., M. A. Kohler, and J. L. H. Paulhus. 1975. Hydrology for engineers. 2nd ed. New  
615 York: McGraw-Hill.

616 Liu, J.Z., A.X. Zhu, Y.B. Liu, T.X. Zhu, and C.Z. Qin. 2014. A layered approach to parallel  
617 computing for spatially distributed hydrological modeling. Environmental Modelling &  
618 Software 51(January):221-227.

619 Liu, J.Z., A.X. Zhu, C.Z. Qin, H. Wu, and J.C. Jiang. 2016. A two-level parallelization method for  
620 distributed hydrological models. Environmental Modelling & Software 80(June):175-184.

621 Liu, Y. B. 2004. Development and application of a GIS-based distributed hydrological model for  
622 flood prediction and watershed management. PhD dissertation, Vrije Universiteit Brussel,  
623 Belgium.

624 Liu, Y. B., S. Gebremeskel, F. De Smedt, L. Hoffmann, and L. Pfister. 2003. A diffusive transport  
625 approach for flow routing in GIS-based flood modeling. Journal of Hydrology 283(1-4):91-

626 106.

627 Maier, H. R., Z. Kapelan, J. Kasprzyk, J. Kollat, L. S. Matott, M. C. Cunha, G. C. Dandy, M. S.  
628 Gibbs, E. Keedwell, A. Marchi, A. Ostfeld, D. Savic, D. P. Solomatine, J. A. Vrugt, A. C.  
629 Zecchin, B. S. Minsker, E. J. Barbour, G. Kuczera, F. Pasha, A. Castelletti, M. Giuliani, and  
630 P. M. Reed. 2014. Evolutionary algorithms and other metaheuristics in water resources:  
631 Current status, research challenges and future directions. *Environmental Modelling &*  
632 *Software* 62 (December):271-299.

633 Maringanti, C., I. Chaubey, M. Arabi, and B. Engel. 2011. Application of a multi-objective  
634 optimization method to provide least cost alternatives for NPS pollution control.  
635 *Environmental Management* 48(3):448-461.

636 Miller, B. A., and R. J. Schaetzl. 2015. Digital classification of hillslope position. *Soil Science*  
637 *Society of America Journal* 79 (January):132-145.

638 Moriasi, D. N., J. G. Arnold, M. W. Van Liew, R. L. Bingner, R. D. Harmel, and T. L. Veith. 2007.  
639 Model evaluation guidelines for systematic quantification of accuracy in watershed  
640 simulations. *Transactions of the ASABE* 50(3):885-900.

641 Mudgal, A., C. Baffaut, S.H. Anderson, E.J. Sadler, and A.L. Thompson. 2010. APEX model  
642 assessment of variable landscapes on runoff and dissolved herbicides. *Transactions of the*  
643 *ASABE* 53(4):1047-1058.

644 Neitsch, S. L., J. G. Arnold, J. R. Kiniry, and J. R. Williams. 2011. Soil and water assessment tool  
645 theoretical documentation version 2009. Texas Water Resources Institute.

646 O'Callaghan, J. F., and D. M. Mark. 1984. The extraction of drainage networks from digital

- 647 elevation data. *Computer Vision, Graphics, and Image Processing* 28(3):323-344.
- 648 Panagopoulos, Y., C. Makropoulos, and M. Mimikou. 2012. Decision support for diffuse pollution  
649 management. *Environmental Modelling & Software* 30(April):57-70.
- 650 Pennock, D.J. 2005. Precision conservation for co-management of carbon and nitrogen on the  
651 Canadian prairies. *Journal of Soil and Water Conservation* 60(6):396-401.
- 652 Priestley, C., and R. Taylor. 1972. On the assessment of surface heat flux and evaporation using  
653 large-scale parameters. *Monthly Weather Review* 100(2):81-92.
- 654 Pyo, J., S.-S. Baek, M. Kim, S. Park, H. Lee, J.-S. Ra, and K. H. Cho. 2017. Optimizing  
655 Agricultural Best Management Practices in a Lake Erie Watershed. *Journal of the American*  
656 *Water Resources Association (JAWRA)*, doi: 10.1111/1752-1688.12571.
- 657 Qin, C.Z., A.X. Zhu, X. Shi, B.L. Li, T. Pei, and C. H. Zhou. 2009. Quantification of spatial  
658 gradation of slope positions. *Geomorphology* 110(3-4):152-161.
- 659 Qin C.Z., A.X. Zhu, W.L. Qiu, Y.J. Lu, B.L. Li, T Pei. Mapping soil organic matter in small low-  
660 relief catchments using fuzzy slope position information. *Geoderma*, 2012, 171-  
661 172(February): 64-74.
- 662 Rodriguez, H. G., J. Popp, C. Maringanti, and I. Chaubey. 2011. Selection and placement of best  
663 management practices used to reduce water quality degradation in Lincoln Lake watershed.  
664 *Water Resources Research* 47(1):1-13.
- 665 Sahu, M., and R.R. Gu. 2009. Modeling the effects of riparian buffer zone and contour strips on  
666 stream water quality. *Ecological Engineering* 35(8):1167-1177.
- 667 Saxton, K.E., and W.J. Rawls. 2006. Soil water characteristic estimates by texture and organic

668 matter for hydrologic solutions. *Soil Science Society of America Journal* 70(5):1569-1578.

669 Schmidt, J., and A. Hewitt. 2004. Fuzzy land element classification from DTMs based on geometry  
670 and terrain position. *Geoderma* 121(3-4):243-256.

671 Srivastava, P., J.M. Hamlett, and P.D. Robillard. 2003. Watershed optimization of agricultural best  
672 management practices: continuous simulation versus design storms. *Journal of the American*  
673 *Water Resources Association (JAWRA)* 39(5):1043-1054.

674 Swanson, F. J., T. K. Kratz, N. Caine, and R. G. Woodmansee. 1988. Landform effects on  
675 ecosystem patterns and processes. *BioScience* 38(2):92-98.

676 Tomer, M.D., S.A. Porter, D.E. James, K.M. Boomer, J.A. Kostel, and E. McLellan. 2013.  
677 Combining precision conservation technologies into a flexible framework to facilitate  
678 agricultural watershed planning. *Journal of Soil and Water Conservation* 68(5):113A-120A.

679 Turpin, N., P. Bontems, G. Rotillon, I. Bärlund, M. Kaljonen, S. Tattari, F. Feichtinger, P. Strauss,  
680 R. Haverkamp, and M. Garnier. 2005. AgriBMPWater: Systems approach to environmentally  
681 acceptable farming. *Environmental Modelling & Software* 20(2):187-196.

682 Veith, T.L., M.L. Wolfe, C.D. Heatwole. 2004. Cost-effective BMP placement: optimization versus  
683 targeting. *Transactions of the ASAE* 47(5):1585-1594.

684 Wang, X.Q. 2008. Comprehensive benefits evaluation of soil erosion control models and  
685 establishing the control paradigm in red soil region. Master dissertation, Huazhong  
686 Agricultural University, Wuhan, China. (in Chinese with English abstract)

687 Williams, J. R. 1975. Sediment-yield prediction with universal equation using runoff energy factor.  
688 *In Present and Prospective Technology for Predicting Sediment Yield and Sources*, 244-252.

689           USDA.

690 Williams, J.R. 1980. SPNM, a model for predicting sediment, phosphorus, and nitrogen yields  
691           from agricultural basins. *Journal of the American Water Resources Association (JAWRA)*  
692           16(5):843-848.

693 Williams, J. R. 1995. The EPIC model. *In Computer models of watershed hydrology.* V. P. Singh,  
694           909-1000. Highlands Ranch, CO, USA: Water Resources Publications.

695 Wu, H., A.X. Zhu, J.Z. Liu, Y.B. Liu, and J.C. Jiang. 2017. Best Management Practices  
696           Optimization at Watershed Scale: Incorporating Spatial Topology among Fields. *Water*  
697           Resources Management, doi: 10.1007/s11269-017-1801-8.

698 Xie, J., C.Z. Qin, G.R. Xiao, L. Yang, Q.L. Lei, J.Z. Liu, and A.X. Zhu. 2015. Soil property  
699           mapping using fuzzy clustering method in small watershed of the red soil region in southern  
700           China: A case study of Zhuxi watershed. *Science of Soil and Water Conservation* 13(5):132-  
701           139. (in Chinese with English abstract)

702 Yang, G.X., and E. P. H. Best. 2015. Spatial optimization of watershed management practices for  
703           nitrogen load reduction using a modeling-optimization framework. *Journal of Environmental*  
704           Management 161(September):252-260.

705 Zitzler, E., M. Laumanns, and L. Thiele. 2001. SPEA2: Improving the strength Pareto evolutionary  
706           algorithm. Zurich, Switzerland: Computer Engineering and Networks Laboratory (TIK)  
707           Department of Electrical Engineering Swiss Federal Institute of Technology (ETH).

708 Zitzler, E., L. Thiele, M. Laumanns, C.M. Fonseca, and V.G. da Fonseca. 2003. Performance  
709           assessment of multiobjective optimizers: An analysis and review. *IEEE Transactions on*

710 Evolutionary Computation 7(2):117-132.  
711 Zitzler, E., and L. Thiele. 1999. Multiobjective evolutionary algorithms: a comparative case study  
712 and the strength Pareto approach. IEEE transactions on Evolutionary Computation 3(4):257-  
713 271.

1 **Table captions**

2 Table 1 A brief description of four BMPs which have been adopted in Changting county and  
3 considered in this study.

4 Table 2 Cost-benefits of four BMPs estimated from local government project (unit: 10,000  
5 RMBY/km<sup>2</sup>).

6 Table 3 Effects of four BMPs on major soil properties and USLE factors after 8 years of  
7 implementation, according to the sample data in Changting county.

8 Table 4 The knowledge on the spatial relationships between BMPs and slope positions.

9

10 **Table 1**

11 A brief description of four BMPs which have been adopted in Changting county and considered  
 12 in this study.

BMP	Brief description
Closing measures (CM)	Facilitate afforestation from human disturbance (e.g., tree felling and grazing). <b>Suitable for the ridge area and upslope positions</b> that suffer low or moderate soil erosion.
Arbor-bush-herb mixed plantation (ABHMP)	Planting trees (e.g., <i>Schima superba</i> and <i>Liquidambar formosana</i> ), bushes (e.g., <i>Lespedeza bicolor</i> ), and herbs (e.g., <i>Paspalum wettsteinii</i> ) in level trenches with compound fertilizer in positions with high-to-violent soil and water losses. <b>Suitable for all slope positions.</b>
Low-quality forest improvement (LQFI)	Improving the infertile forest by applying compound fertilizer to every hole (40 cm × 40 cm × 40 cm) in the uphill position of crown projection. Suitable for the moderate or serious eroded land in <b>the upslope and steep backslope positions.</b>
Orchard improvement (OI)	Constructing level terraces, drainage ditches, storage ditches, irrigation facilities and roads, planting economic fruit, and interplanting grasses and Fabaceae ( <i>Leguminosae</i> ) plants in orchards <b>on the middle and down slope positions</b> under better water and fertilizer conditions.

13

14

15 **Table 2**

16 Cost-benefits of four BMPs estimated from local government project (unit: 10,000 RMBY/km<sup>2</sup>)

BMP	Implementation cost	Annual maintenance cost	Annual benefit
CM	15.5	1.5	2.0
ABHMP	87.5	1.5	6.9
LQFI	45.5	1.5	3.9
OI	420	20	60.3

17 Notes: CM = Closing measures, ABHMP = Arbor-bush-herb mixed plantation, LQFI = Low-quality forest  
18 improvement, OI = Orchard improvement.

19 Source: Wang (2008)

20

21 **Table 3**

22 Effects of four BMPs on major soil properties and USLE factors after 8 years of implementation,  
 23 according to the sample data in Changting county.

BMP	OM*	BD	PORO†	SOL_K	USLE_K‡	USLE_P‡
CM	1.22	0.98	1.02	0.81	1.01	0.90
ABHMP	1.45	0.93	1.07	1.81	0.82	0.50
LQFI	1.05	0.87	1.13	1.71	0.81	0.50
OI	2.05	0.96	1.03	1.63	0.88	0.75

24 Notes: Values in table are relative changes (i.e., multiply) corresponding to the original properties.

25 CM = Closing measures, ABHMP = Arbor-bush-herb mixed plantation, LQFI = Low-quality forest  
 26 improvement, OI = Orchard improvement, OM = Organic matter, BD = Bulk density, PORO = Total porosity,  
 27 SOL\_K = Soil hydraulic conductivity.

28 \* The effect on organic matter is the same as on soil organic carbon.

29 † The effect on total porosity is the same as on field capacity, wilting point, etc.

30 ‡ USLE\_K and USLE\_P are soil erodibility factor and conservation practice factor, respectively.

31

32

33 **Table 4**

34 The knowledge on the spatial relationships between BMPs and slope positions.

BMP	Suitable slope positions	Suitable landuses	Effectiveness grade
CM	ridge, backslope	forest	3
ABHMP	ridge, backslope, and valley	forest, orchard	5
LQFI	backslope	forest	4
OI	valley	forest, orchard	4

35 Notes: CM = Closing measures, ABHMP = Arbor-bush-herb mixed plantation, LQFI = Low-quality forest  
 36 improvement, OI = Orchard improvement

37

38

## 1 **Figure captions**

2 Figure 1 Illustration of an integrated management scheme for soil and water conservation in  
3 southeast China (adapted from Cai et al. (2012)).

4 Figure 2 The proposed framework for the spatial optimization of watershed BMPs based on slope  
5 position units.

6 Figure 3 Map of the Youwuzhen watershed in Fujian province, China.

7 Figure 4 Slope position units delineated in the Youwuzhen watershed.

8 Figure 5 Calibration (a) and validation (b) of the simulated flow discharge ( $\text{m}^3/\text{s}$ ) at the watershed  
9 outlet of the study area.

10 Figure 6 Calibration (a) and validation (b) of the simulated sediment export (kg) at the watershed  
11 outlet of the study area.

12 Figure 7 Near Pareto optimal solutions derived from the first to 100<sup>th</sup> generation by the proposed  
13 approach (a) and the random approach (b).

14 Figure 8 Changes in the hypervolume index with generations by the proposed approach and the  
15 random approach, respectively.

16 Figure 9 Comparison of near Pareto optimal solutions by the proposed approach and the random  
17 approach under different generations (a: the first generation, b: the 10<sup>th</sup> generation, c: the 35<sup>th</sup>  
18 generation, d: the 100<sup>th</sup> generation).

19 Figure 10 Comparison of the BMP scenarios selected randomly from the near Pareto optimal  
20 solutions of the 10<sup>th</sup> generation from the proposed approach (a: 32.4% reduction rate of soil  
21 erosion and 0.51 million RMBY net cost) and the random approach (b: 21.2% reduction rate

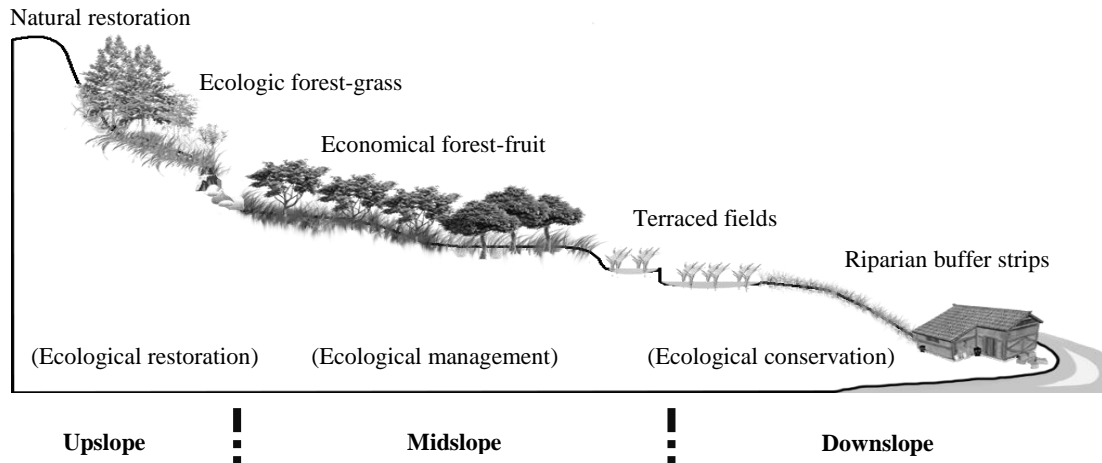
22 of soil erosion and 0.53 million RMBY net cost), respectively. (CM = Closing measures,  
23 ABHMP = Arbor-bush-herb mixed plantation, LQFI = Low-quality forest improvement, OI  
24 = Orchard improvement.)

25 Figure 11 Comparison of the BMP scenarios selected randomly by the near Pareto optimal  
26 solutions of the 100<sup>th</sup> generation from the proposed approach (a: 47.7% reduction rate of soil  
27 erosion and 1.22 million RMBY net cost) and the random approach (b: 47.9% reduction rate  
28 of soil erosion and 1.15 million RMBY net cost), respectively. (CM = Closing measures,  
29 ABHMP = Arbor-bush-herb mixed plantation, LQFI = Low-quality forest improvement, OI  
30 = Orchard improvement.)

31

32 **Figure 1**

33 Illustration of an integrated management scheme for soil and water conservation in southeast  
34 China (adapted from Cai et al. (2012)).



35

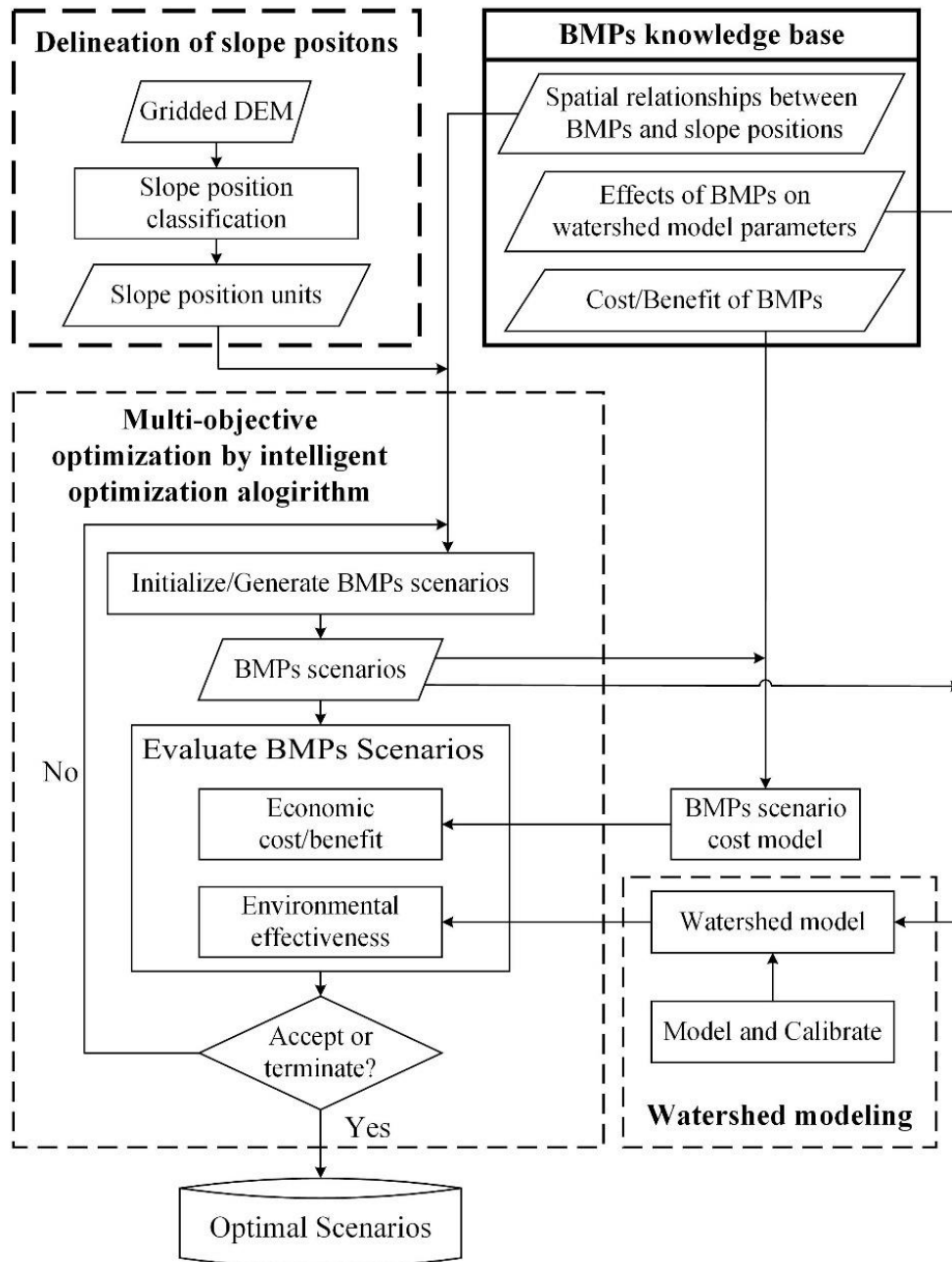
36

37

38 **Figure 2**

39 The proposed framework for the spatial optimization of watershed BMPs based on slope position

40 units.

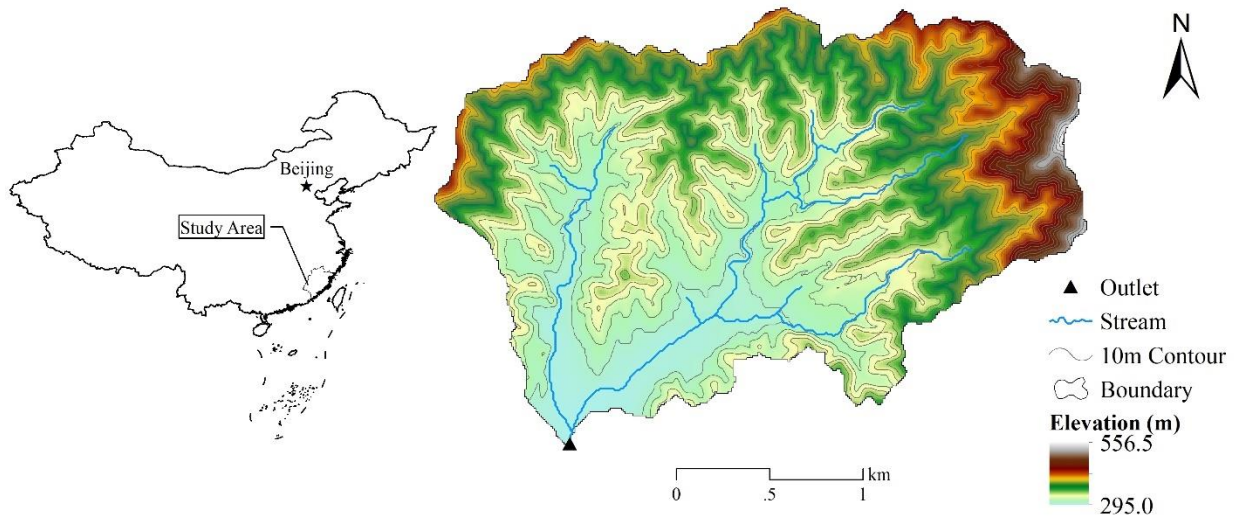


41

42

43 **Figure 3**

44 Map of the Youwuzhen watershed in Fujian province, China.



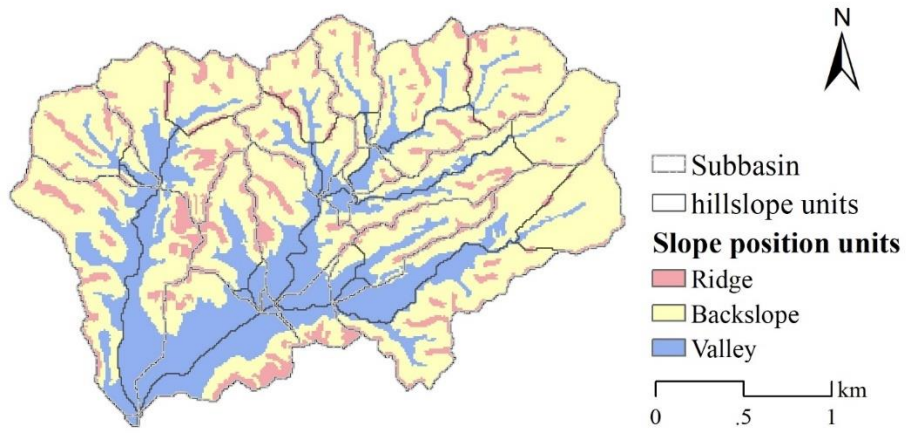
45

46

47

48 **Figure 4**

49 Slope position units delineated in the Youwuzhen watershed.



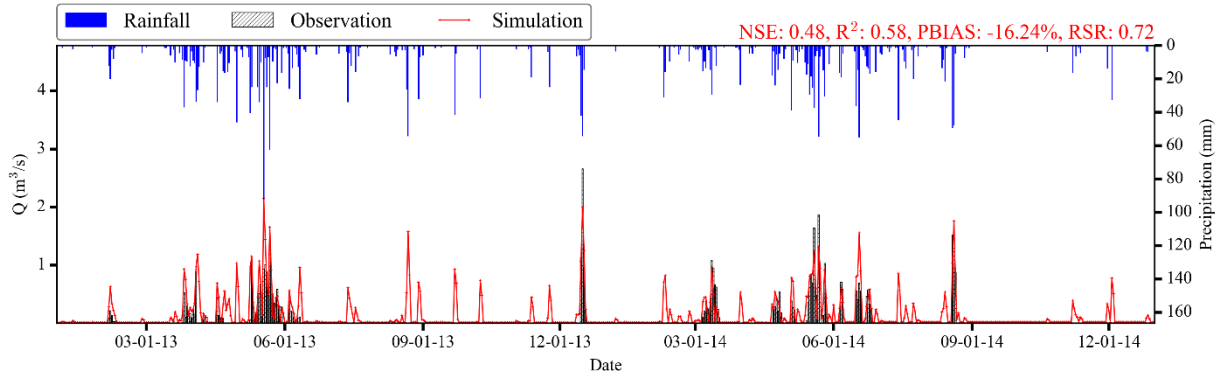
50

51

52

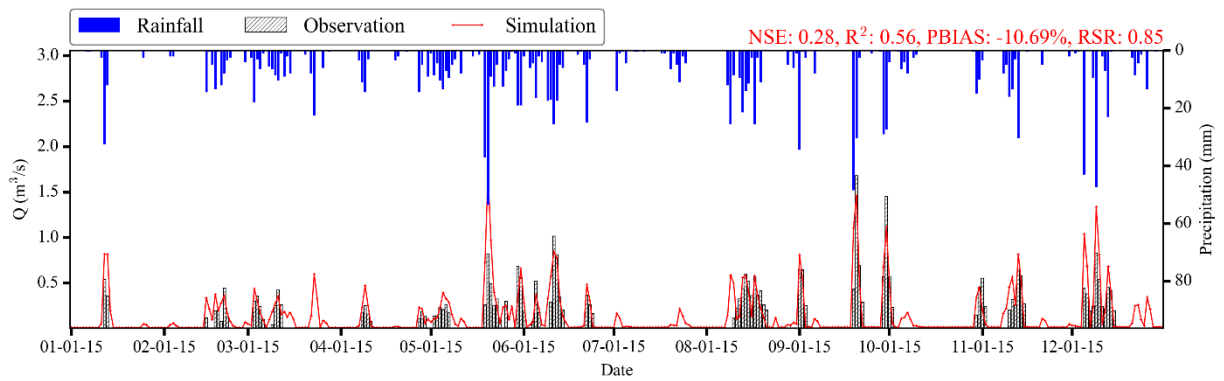
53 **Figure 5**

54 Calibration (a) and validation (b) of the simulated flow discharge ( $\text{m}^3/\text{s}$ ) at the watershed outlet of  
55 the study area.



56  
57

(a)

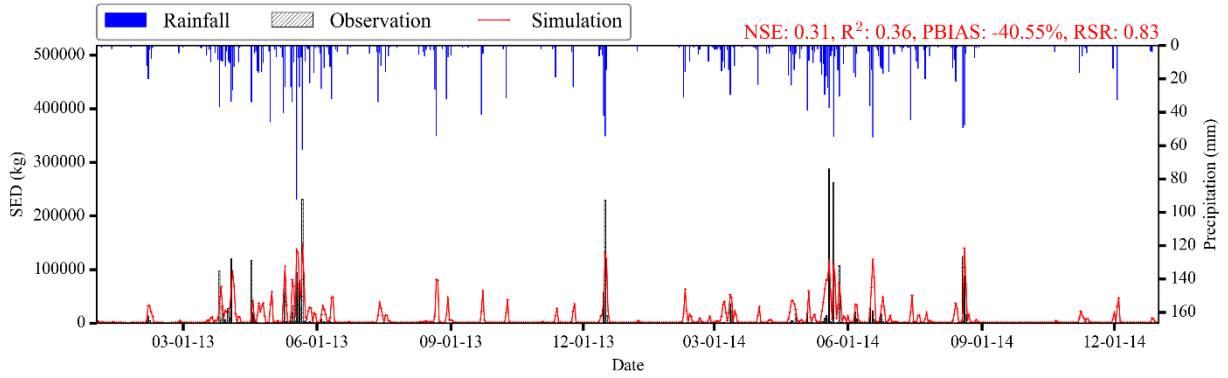


58  
59  
60

(b)

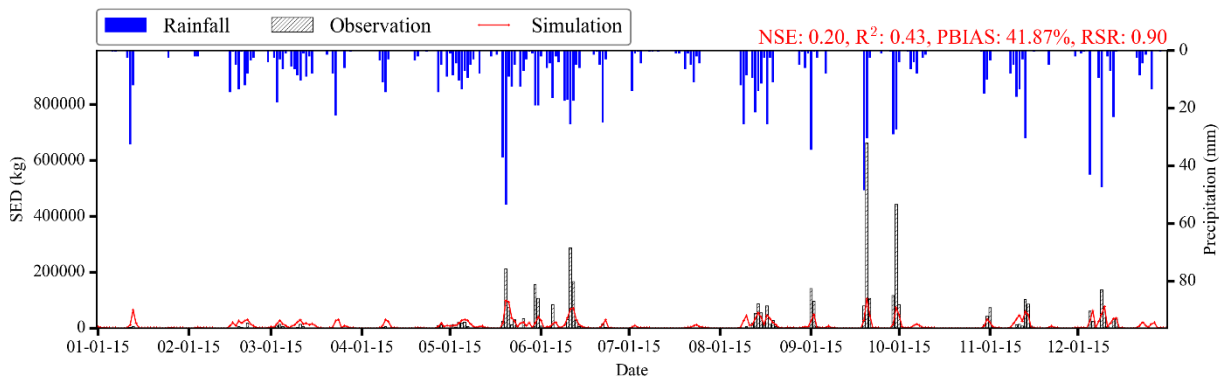
61 **Figure 6**

62 Calibration (a) and validation (b) of the simulated sediment export (kg) at the watershed outlet of  
63 the study area



64  
65

(a)



66  
67  
68

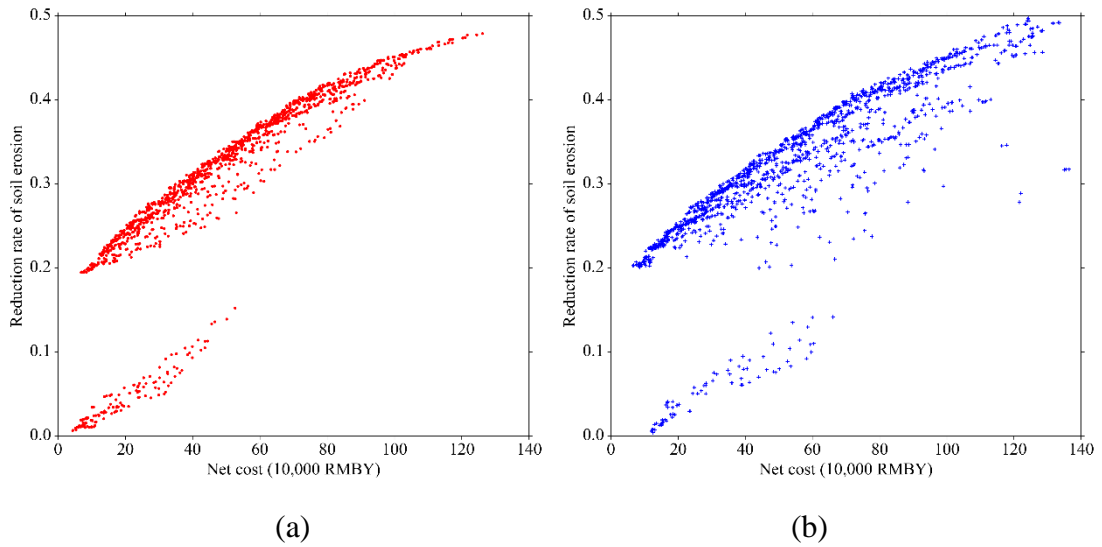
(b)

69 **Figure 7**

70 Near Pareto optimal solutions derived from the first to 100<sup>th</sup> generation by the proposed approach

71 (a) and the random approach (b).

72



73

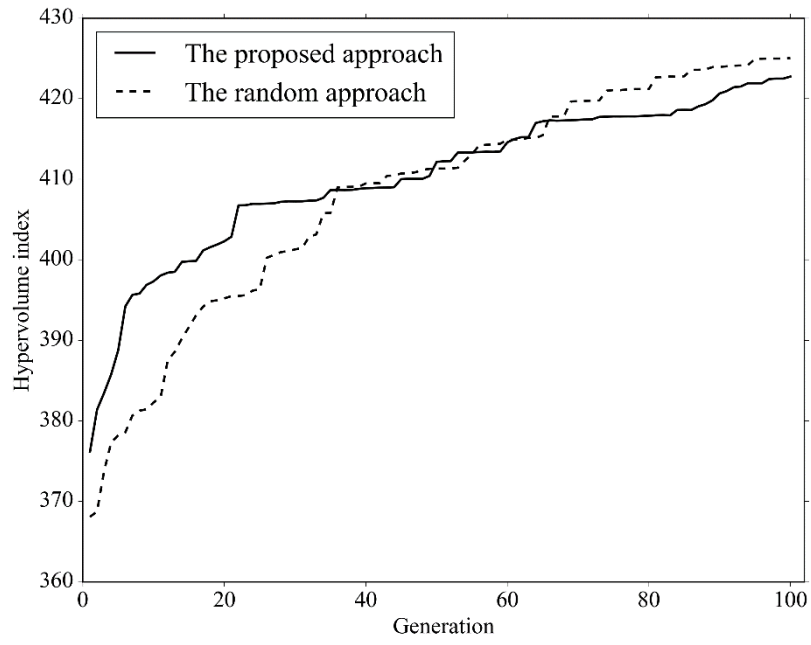
74

75

76

77 **Figure 8**

78 Changes in the hypervolume index with generations by the proposed approach and the random  
79 approach, respectively.



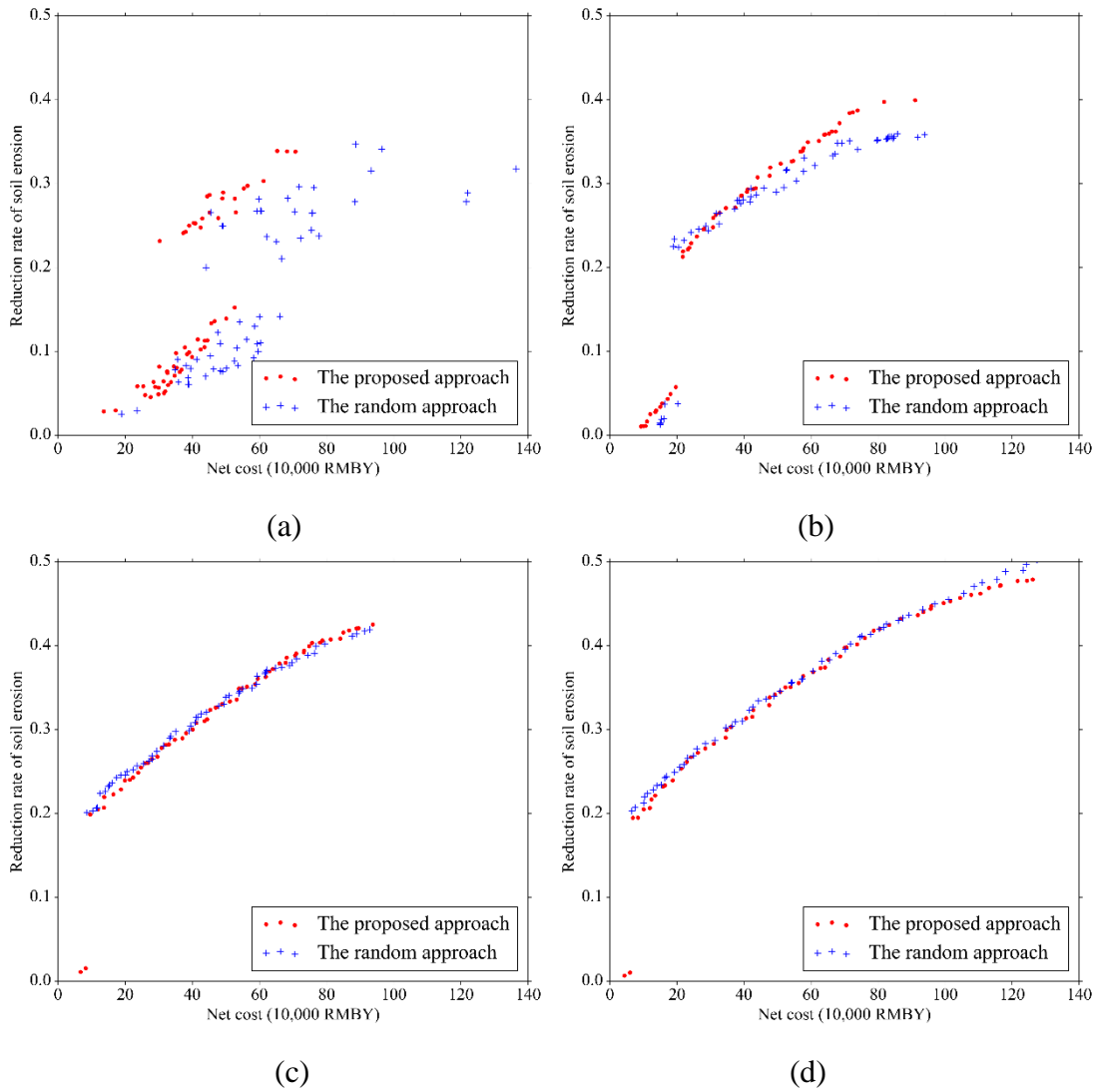
80

81

82

83 **Figure 9**

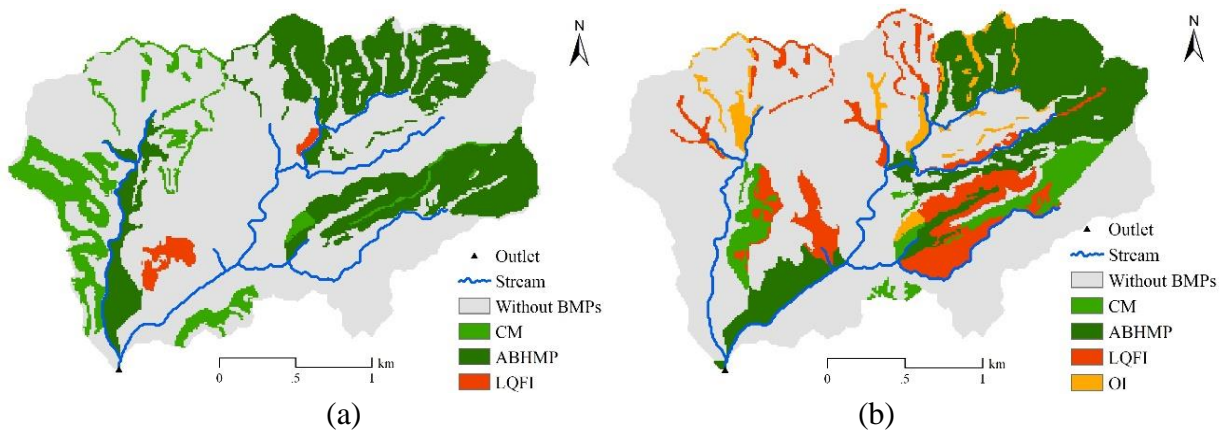
84 Comparison of near Pareto optimal solutions by the proposed approach and the random approach  
85 under different generations (a: the first generation, b: the 10<sup>th</sup> generation, c: the 35<sup>th</sup> generation, d:  
86 the 100<sup>th</sup> generation).



89  
90  
91  
92

93 **Figure 10**

94 Comparison of the BMP scenarios selected randomly from the near Pareto optimal solutions of the  
95 10<sup>th</sup> generation from the proposed approach (a: 32.4% reduction rate of soil erosion and 0.51  
96 million RMBY net cost) and the random approach (b: 21.2% reduction rate of soil erosion and  
97 0.53 million RMBY net cost), respectively. (CM = Closing measures, ABHMP = Arbor-bush-herb  
98 mixed plantation, LQFI = Low-quality forest improvement, OI = Orchard improvement.)



102 **Figure 11**

103 Comparison of the BMP scenarios selected randomly by the near Pareto optimal solutions of the  
104 100<sup>th</sup> generation from the proposed approach (a: 47.7% reduction rate of soil erosion and 1.22  
105 million RMBY net cost) and the random approach (b: 47.9% reduction rate of soil erosion and  
106 1.15 million RMBY net cost), respectively. (CM = Closing measures, ABHMP = Arbor-bush-herb  
107 mixed plantation, LQFI = Low-quality forest improvement, OI = Orchard improvement.)

